Interaction of Polycationic Polymers with Supported Lipid Bilayers and Cells: Nanoscale Hole Formation and Enhanced Membrane Permeability

Seungpyo Hong,[||,#,†] Pascale R. Leroueil,[⊥,#,†] Elizabeth K. Janus,[§,#] Jennifer L. Peters,[#] Mary-Margaret Kober,[⊥,#] Mohammad T. Islam,[#] Bradford G. Orr,[‡,⊗,#] James R. Baker, Jr.,[#] and Mark M. Banaszak Holl[‡,§,||,⊥,#,*]

Programs in Applied Physics, Biophysics, and Macromolecular Science and Engineering, Departments of Chemistry and Physics, and Michigan Nanotechnology Institute for Medicine and Biological Sciences, University of Michigan, Ann Arbor, Michigan 48109. Received March 27, 2006; Revised Manuscript Received April 5, 2006

Interactions of polycationic polymers with supported 1,2-dimyristoyl-sn-glycero-3-phosphocholine (DMPC) lipid bilayers and live cell membranes (KB and Rat2) have been investigated using atomic force microscopy (AFM), cytosolic enzyme assays, confocal laser scanning microscopy (CLSM), and a fluorescence-activated cell sorter (FACS). Polycationic polymers poly-L-lysine (PLL), polyethylenimine (PEI), and diethylaminoethyl-dextran (DEAE-DEX) and sphere-like poly(amidoamine) (PAMAM) dendrimers are employed because of their importance for gene and drug delivery. AFM studies indicate that all the polycationic polymers cause the formation and/or expansion of preexisting defects in supported DMPC bilayers in the concentration range of 1−3 μg/mL. By way of contrast, hydroxyl-containing neutral linear poly(ethylene glycol) (PEG) and poly(vinyl alcohol) (PVA) do not induce hole formation or expand the size of preexisting defects in the same concentration range. All polymers tested are not toxic to KB or Rat2 cells up to a 12 μg/mL concentration (XTT assay). In the concentration range of 6−12 μg/mL, however, significant amounts of the cytosolic enzymes lactate dehydrogenase (LDH) and luciferase (LUC) are released. PEI, which possesses the greatest density of charged groups on its chain, shows the most dramatic increase in membrane permeability. In addition, treatment with polycationic polymers allows the small dye molecules propidium idodide (PI) and fluorescein (FITC) to diffuse in and out of the cells. CLSM images also show internalization of PLL labeled with FITC dye. In contrast, controls of membrane permeability using the neutral linear polymers PEG and PVA show dramatically less LDH and LUC leakage and no enhanced dye diffusion. Taken together, these data are consistent with the hypothesis that polycationic polymers induce the formation of transient, nanoscale holes in living cells and that these holes allow a greatly enhanced exchange of materials across the cell membrane.

INTRODUCTION

The water soluble synthetic polycationic polymers poly-L-lysine (PLL), polyethylenimine (PEI), diethylaminoethyl-dextran (DEAE-DEX), and polyamidoamine (PAMAM) dendrimers have been employed in a variety of gene and drug delivery system applications (*1*−*3*). The generally accepted mechanism for internalization of these polymers is polycation-mediated endocytosis, a three-step process composed of binding with phospholipids and/or glycolipids in the membrane, internalization into cells, and exit from the endosome (*4*−*7*). Having particular interest in the first step of the process, several research groups have used model systems including phosphatidylethanolamine containing anionic vesicles to study the membrane/particle interaction (*8*−*10*). Studies of model systems have provided good evidence for membrane disruption caused by cationic macromolecules such as PEI, PAMAM dendrimers, and poly-(*N*-ethyl-4-vinylpyridinium bromide) as measured by changes in fluorescence intensity of artificial vesicles containing dyes such as fluorescein (FITC) after exposure to the polycations (*10*−*12*). Several reports using living cell membranes have also demonstrated increased membrane permeability as determined by cytotoxicity (cytosolic enzyme leakage such as LDH) using assay techniques (*13*, *14*). However, no clear connection has been made between proposed models and in vitro studies.

We recently reported that positively charged PAMAM dendrimers cause membrane disruption (dendroporation), allowing the diffusion of molecules in and out of cells (*15*). This in vitro result is in good agreement with the proposed hole formation mechanism, as suggested by atomic force microscopy (AFM) on a supported 1,2-dimyristoyl-sn-glycero-3-phosphocholine (DMPC) model membrane (*16*−*19*). On the basis of our previous results, we wanted to explore if nanoscale hole formation could be caused by less exotic polycationic polymers such as PEI, PLL, and DEAE-DEX which are substantially cheaper and more commonly used materials than the PAMAM dendrimers. The key hypotheses we address in this paper are as follows:

(1) Commercially available polycationic polymers, PEI, PLL, and DEAE-DEX cause nanoscale hole formation in supported lipid bilayers.

(2) Commercially available polycationic polymers, PEI, PLL, and DEAE-DEX cause substantial permeability of the cell plasma membrane allowing enhanced enzyme and dye diffusion.

(3) Under the same conditions, neutral linear polymers (PEG and PVA) do not cause nanoscale hole formation in supported lipid bilayers nor do they generate comparable enhancements in cell membrane permeability.

In this study, we employed AFM to observe the effect of

* To whom correspondence should be addressed. Phone: (734) 763-2283. Fax: (734) 763-2307. E-mail: mbanasza@umich.edu.

‡ Program in Applied Physics.

§ Program in Biophysics.

|| Program in Macromolecular Science and Engineering.

⊥ Department of Chemistry.

⊗ Department of Physics.

Michigan Nanotechnology Institute for Medicine and Biological Sciences.

† Both authors provided the same contribution for this work.

10.1021/bc060077y CCC: $33.50
Published on Web 05/02/2006

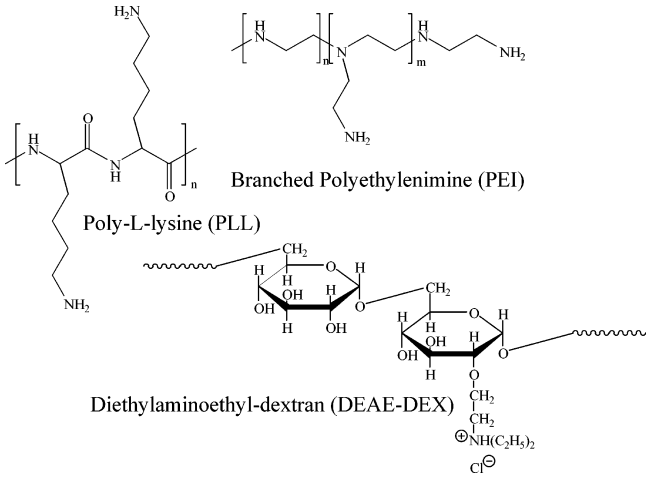

Figure 1. Chemical structures of commercially available polycationic polymers used in this study.

polymers upon supported DMPC lipid bilayers. Polymer interactions with cells in vitro were investigated in terms of morphological studies using confocal laser scanning microscopy (CLSM) as well as toxicological studies using XTT, lactate dehydrogenase (LDH), and luciferase (LUC) assays and flow cytometry. AFM studies revealed that the presence of polycationic polymers induces nanoscale hole formation and/or the expansion of preexisting defects in the supported DMPC bilayers. The presence of polycationic polymers in the cell medium made the cell membrane permeable to molecules such as cytosolic enzymes (LDH and LUC), propidium iodide (PI), and FITC. These results directly support the three hypotheses described above and suggest an alternative model to polycation-mediated endocytosis for the transport of materials across cell membranes in the presence of polycationic polymers.

EXPERIMENTAL PROCEDURES

Materials and Measurement of Molar Masses. PLL, PLL−FITC conjugate (PLL−FITC), PEI, and DEAE-DEX were purchased from Sigma-Aldrich. G5 PAMAM dendrimers were synthesized and then conjugated with FITC at the Michigan Nanotechnology Institute for Medicine and Biological Sciences, University of Michigan (*15*). DMPC lipids were provided by Avanti Lipids, Alabaster, AL. Chemical structures of the polycationic polymers used in this paper are illustrated in Figure 1.

The molar mass moments and molar mass distribution of each polymer sample was measured using gel permeation chromatography (GPC). The number average molar mass (M_n) and polydispersity index (PDI), a commonly used measure of the breadth of the molar mass distribution defined as the ratio of the weight and number average molar masses (M_w/M_n), of individual samples are listed in Table 1. GPC experiments were performed using an Alliance Waters 2690 separation module (Waters Corp., Milford, MA) equipped with a Waters 2487 UV absorbance detector (Waters Corp.), a Wyatt Dawn DSP laser photometer (Wyatt Technology Corp., Santa Barbara, CA), an Optilab DSP interferometric refractometer (Wyatt Technology Corp.), and TosoHaas TSK-Gel Guard PHW 06762 (75×7.5 mm, 12 μm), G 2000 PW 05761 (300 × 7.5 mm, 10 μm), G 3000 PW 05762 (300 × 7.5 mm, 10 μm), and G 4000 PW (300 × 7.5 mm, 17 μm) columns. Column temperatures were maintained at 25 ± 0.2 °C with a Waters temperature control module. Citric acid buffer (0.1 M) with 0.025% sodium azide in water was used as a mobile phase. The pH of the mobile phase was adjusted to 2.74 using NaOH, and the flow rate was maintained at 1 mL/min. Sample concentration was approximately 2 mg/mL, and an injection volume of 100 μL was used for all samples. Molar mass moments of the polymers were determined using Astra software (version 4.7) (Wyatt Technology Corp.).

Preparation and AFM Observation of Supported DMPC Lipid Bilayers. A 0.67 mg/mL suspension of small, unilamellar vesicles (SUVs) was prepared as previously reported (*15, 16, 20*). Supported lipid bilayers were formed by depositing 80 μL of liposome suspension on a 1 × 1 cm^2 piece of freshly cleaved mica. After an incubation time of approximately 20 min, the sample was gently rinsed with water to remove excess lipids and placed in the AFM for imaging as described in previous studies. All AFM measurements were performed in tapping mode on a Nanoscope IIIa Multimode scanning probe microscope from Digital Instruments (DI, Veeco Metrology Group, Santa Barbara, CA). The AFM was equipped with a liquid cell (DI) and a silicon nitride cantilever (DI model NPS, spring constant 0.32 N/m, length 100 μm) operating at a drive frequency of 6−9 kHz. After taking an initial image of the bilayer, approximately 20 μL of polymer solution was injected into the liquid cell. All solutions were prepared using high purity water (Nerl Diagnostics, East Providence, RI). The temperature inside the liquid cell was 28 °C and therefore above the gel to liquid transition temperature of supported DMPC bilayers.

Cell Lines. The KB and Rat2 cell lines were purchased from the American Type Tissue Collection (ATCC, Manassas, VA) and grown continuously as a monolayer at 37 °C and 5% CO_2 in RPMI 1640 medium (Mediatech, Herndon, VA) and Dulbecco's modified Eagle's medium (DMEM, Gibco, Eggenstein, Germany), respectively. The Rat2 cell line was transfected to permanently express the LUC gene using PAMAM dendrimer-mediated gene transfection as previously described (*15, 21, 22*). The LUC expressing Rat2 cells are noted as Rat2pLUC. The RPMI 1640 and DMEM media were supplemented with penicillin (100 units/mL), streptomycin (100 μg/mL), and 10% heat-inactivated fetal bovine calf serum (FBS) before use.

XTT, LUC, and LDH Assays and Flow Cytometry. Cytotoxicity of the polycationic polymers was assessed with a 2,3-bis(2-methoxy-4-nitro-5-sulfophenyl)-5-[(phenylamino)carbonyl]-*2H*-tetrazolium hydroxide (XTT) assay kit (Cell Proliferation Kit II, Roche Molecular Biochemicals, Mannheim, Germany). KB and Rat2 cell lines (at a concentration of 5 × 10^4 cells/well) were prepared as monolayers in 96 well plates, followed by incubation with polymers in phosphate-buffered saline (PBS) with Ca^{2+} and Mg^{2+} at 37 °C under 5% CO_2 for 4.5 h. Polymer solutions (supernatants) were removed and followed by washing with PBS twice. Mitochondrial activities in the cells were then measured using the assay kit.

The LDH and LUC activities in the cell supernatant after 3 h incubation were respectively analyzed using an LDH assay kit (Promega Co., Madison, WI) and a chemiluminescence assay(Promega Co., Madison, WI) as previously described (*15*). The measured LDH and LUC activities were either recalculated by percentage to the activities of cell lysates of intact cells (% LDH released) or adjusted for the protein concentration of the sample (relative light unit (RLU)/mg protein). Flow cytometry was also performed according to our report (*15*). Fluorescence signal intensities were measured by a Coulter EPICS/XL MCL Beckman-Coulter flow cytometer and data were analyzed using Expo32 software (Beckman-Coulter, Miami, FL).

CLSM Observation. A concentration of 2 × 10^4 cells/mL of Rat2 cells was seeded on MatTek glass bottom Petri dishes (35 mm) and incubated at 37 °C under 5% CO_2 for 24 h. The DMEM was removed and 2 mL of each PLL−FITC and dendrimer−FITC conjugates in PBS (Ca^{2+}, Mg^{2+}) solution was added into the appropriate dish. The dishes were incubated with added solutions at 37 °C under 5% CO_2 for 1 h. The conjugate-

Table 1. Physicochemical Properties of Polycations Used in This Study

polymer	M_n (PDI)[a]	order of amines (deg)	charge/monomer ratio[b]	zeta potential (mV)[c]	shape of chain
PLL	11210 (1.67)	1, 2	0.007519	17.59 ± 0.39	linear, flexible
PLL−FITC	23620 (1.06)	1, 2	0.007519	-	linear, flexible
PEI	78220 (3.44)	1, 2, 3	0.02290	45.18 ± 16.84	branched, flexible
DEAE-DEX	18490 (32.90)	3	0.00218	30.44 ± 2.71	linear, intramolecular cross-linking
G5-NH_2	26530 (1.02)	1, 3	0.00885	19.24 ± 16.63	sphere-like
PEG	16290 (1.22)	N/A	N/A	−1.07 ± 1.10	linear, flexible
PVA	28490 (1.57)	N/A	N/A	−0.68 ± 1.36	linear, inter-/intramolecular H bonding

[a] Measured by GPC. [b] Theoretical number of charged groups per molecular weight of polymeric monomer. [c] Measured by zeta potential/particle sizer NICOMP 380 ZLS (PSS·NICOMP, Santa Barbara, CA). The maximum count rate was 5 MHz and the measurements were carried out for 5 min. All the polymer samples were at a concentration of 1 mg/mL, pH 7.4, and measurements for each polymer were repeated five times.

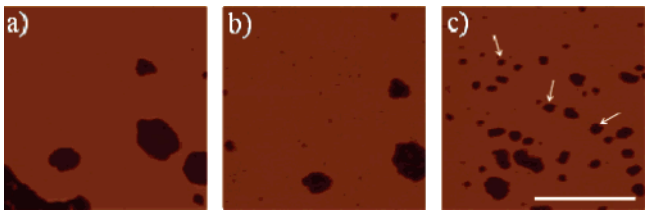

Figure 2. AFM images of supported DMPC lipid bilayers upon exposure to poly-L-lysine (PLL). 20 μL of 10 μg/mL PLL injected following image a, resulting in a final concentration of ~1.0 μg/mL in the AFM liquid cell. Total time between a and c is approximately 50 min. White arrows indicate formation of several new holes in the lipid bilayers caused by PLL. Bar: 500 nm. Z-scale: 20 nm.

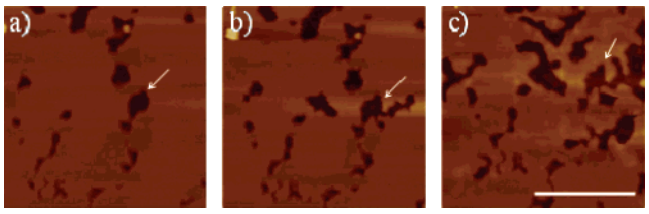

Figure 3. AFM images of supported DMPC lipid bilayers upon exposure to poly(ethylenimine) (PEI). 20 μL of 5 μg/mL PEI injected following image a, resulting in a final concentration of ~0.5 μg/mL. An additional 20 μL of 10 μg/mL was injected after b, resulting in a final concentration of ~1.5 μg/mL. Total time between a and c is approximately 40 min. Note that there is no new hole formation but instead the preexisting defects are expanded. One of the preexisting defects and expansion of the defect is indicated by white arrows in each image. Bar: 500 nm. Z-scale: 20 nm.

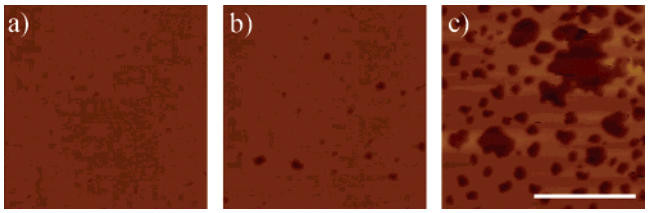

Figure 4. AFM images of supported DMPC lipid bilayers upon exposure to diethylaminoethyl-dextran (DEAE-DEX). 50 μL of 5 μg/mL DEAE-DEX injected following image a, resulting in a final concentration of ~1.3 μg/mL. Total time between a and c is approximately 90 min. Unlike that PLL and PEI create or expand defects in the lipid bilayers, DEAE-DEX induces membrane thinning. The newly formed defects are 2−4 nm deep instead of complete removal of the lipid bilayers (~4−5 nm deep). Bar: 500 nm. Z-scale: 20 nm.

containing solutions were removed, and the resulting cell monolayer was washed with PBS. Cells were fixed with 2% formaldehyde in the PBS (Ca^{2+}, Mg^{2+}) at room temperature for 10 min, followed by washing with PBS twice. Confocal and differential interference contrast (DIC) images were taken on an Olympus FV-500 confocal microscope using a 40×, 1.2 NA oil immersion objective. For the confocal images, the 488 nm line of an argon ion laser was used for excitation and the emission was filtered at 505 nm.

RESULTS

Polycation-Induced Hole Formation on Aqueous Supported DMPC Lipid Bilayers. The polycation polymers used in this study (PLL, PEI, and DEAE-DEX) were all shown to disrupt DMPC-supported lipid bilayers. Several controls were performed for the AFM study. Before the introduction (through injection) of polymers into the solution containing the aqueous supported lipid bilayers, the bilayers were imaged alone for 8 to 10 min. These preimaging steps were done to ensure that the bilayers were stable and that preexisting defects that appeared were not due to the act of imaging itself. A blank injection of water (the solvent in which the polymers were dissolved) was completed and resulted in no change to the bilayer over the course of a normal imaging session (60 to 90 min). This shows that the injection itself is not responsible for the formation of defects. Finally, injections of 1 μg/mL of poly(ethylene glycol) (PEG) and poly(vinyl alcohol) (PVA), two neutral polymers, were performed and resulted in no change to the supported bilayers over normal imaging time.

Images taken using AFM show the three polycationic polymers (PEI, PLL, and DEAE-DEX) disrupt DMPC supported lipid bilayers. Figures 2, 3, and 4 are representative data sets of the polycationic polymers and DMPC lipid bilayer interactions. Although there is some variation, several repetitions were completed for each polymer confirming that the degrees of membrane/polymer interactions are qualitatively similar. Following the addition through injection of PLL into the AFM liquid cell at a final concentration of ~ 1 ug/mL (Figure 2), new defects in the bilayer are formed. The depth of these defects in the membrane is primarily in the range of 4.0−4.8 nm. Addition of PEI onto the bilayer, however, results in mostly the expansion of preexisting defects (Figure 3). These expanded defects have measured 4.4 to 5.1 nm in depth which is consistent with the removal of a full bilayer. Interestingly, the introduction of DEAE-DEX to supported DMPC bilayers results in only 2−4 nm deep depressions.

Cytotoxicity of Polycation and Polycation-Induced Enzyme Leakage. The cytotoxicity of the polymers was determined using an XTT assay (Figure 5). The relative cell viability was calculated as:

$$[OD_{492nm}]_{sample}/[OD_{492nm}]_{control} \times 100$$

The assay results show that the polymers are not cytotoxic up to a 12 μg/mL concentration (>80% cell viability) for both KB and Rat2 cells. Based on these data, the assays performed to investigate the cytosolic enzyme release were carried out in polymer concentrations of 6 and 12 μg/mL. Within this range, the polymers are noncytotoxic, so the observed enzyme release can be ascribed to an increase in cell membrane permeability as opposed to general lysis due to cell death.

The effect of positively charged polymers on the cell membranes was investigated in terms of cytosolic enzyme release from the cells using LDH and LUC assay techniques.

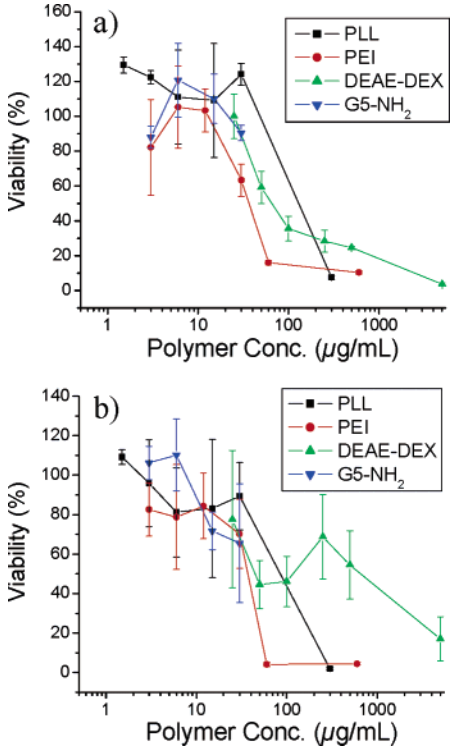

Figure 5. Cell viability determined by XTT assay of (a) KB and (b) Rat2 cells after incubation with PLL, PEI, DEAE-DEX, and G5-NH_2 PAMAM at 37 °C for 4.5 h. Note that all the polymers are not cytotoxic up to a concentration of 12 μg/mL.

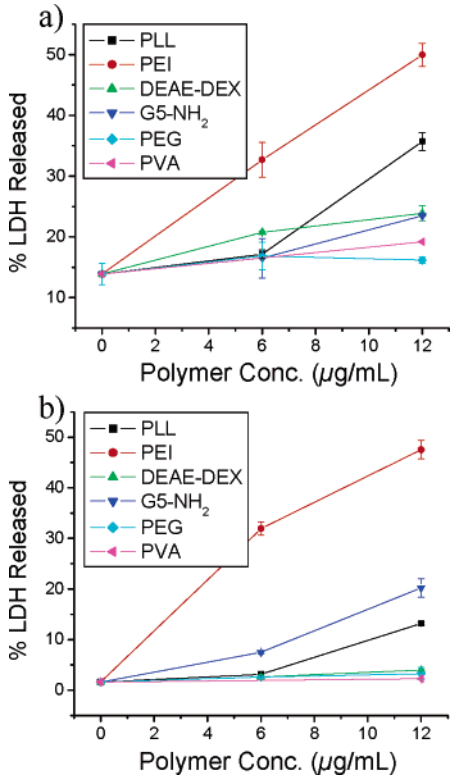

Figure 6. Dose-dependent LDH release from (a) KB and (b) Rat2 cell lines incubated with PLL, PEI, DEAE-DEX, G5-NH_2 PAMAM, PEG, and PVA at 37 °C for 3 h. All the polycationic polymers induce LDH leakage but the neutral polymers PEG and PVA do not cause any significant leakage.

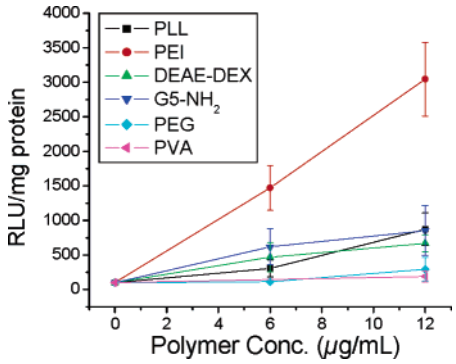

Figure 7. Dose-dependent luciferase (LUC) release from Rat2pLUC cell line incubated with PLL, PEI, DEAE-DEX, G5-NH_2 PAMAM, PEG, and PVA at 37 °C for 3 h. Before the incubation, Rat2 cells were transfected by PAMAM dedrimer-mediated cell transfection to express LUC in their cytosols. As seen in the LDH assay data in Figure 6, all the polycationic polymers used in this study also cause LUC leakage but the neutral polymers do not.

As the polymer concentration increases, the amounts of both LDH and LUC released increased as illustrated in Figures 6 and 7. Induced membrane permeability as measured by LDH release shows a degree of cell type (KB and Rat2) dependence as shown in Figure 6. In both cell types (Figure 6), however, PEI induced more LDH leakage as compared to the other polycationic polymers. This is not surprising because PEI possesses a much greater charge/monomer ratio (see Table 1) as compared to the other polymers. G5-NH_2 and PLL cause similar amount of LDH release and the least LDH was released from the cells after exposure to DEAE-DEX among the polycationic polymers, particularly in the case of the Rat2 cells. PEG and PVA did not cause enzyme leakage. LUC release from Rat2pLUC exhibits a trend similar to the LDH release from cells seen as discussed above (Figure 7).

Binding and Internalization of PLL−FITC. PLL−FITC conjugate was used for direct observation by CLSM. This experiment was carried out to compare the internalization behavior of common commercial polycationic polymers to that of dendrimeric G5-NH_2. Figure 8 shows that PLL−FITC is internalized into the Rat2 cells resulting in strong fluorescence of FITC from inside the cells. In particular, the intracellular location of the internalized conjugates appears to exclude the nucleus. This internalization behavior is particularly interesting because penetration of the polymers into the nucleus should be avoided for nontoxic gene delivery as it may alter the DNA sequence. G5-Ac−FITC, which remains neutral in water due to the conversion of all the surface primary amines groups to acetamide groups, is not internalized as shown in Figure 8e, allowing the conjugate to be used as a negative control (*15*). The DIC image is provided to show that an appropriate cell density was used (Figure 8f).

Diffusion of Small Molecules through the Permeabilized Membranes. It is known that PI and fluorescein diacetate (FDA) can be employed as indicators of diffusion-in and out, respectively (*15*, *23*). PI is readily internalized into cells with disrupted membranes but is excluded from cells with intact membranes. In contrast, FDA is able to traverse intact membranes and is then converted to fluorescein (FITC) by endogenous esterase in cells. The resulting FITC is unable to travel across intact membranes but is able to traverse permeabilized membrane. Therefore, it is assumed that PI fluorescence should increase and FITC fluorescence should decrease with increasing membrane permeability. Figure 9a shows the increase in PI signal intensity induced following the incubation of KB cells with the polycationic polymers. The greatest PI intensity increase is seen using PEI, followed by G5, DEAE-DEX, and PLL. Charge neutral PVA and PEG do not induce PI internalization.

On the other hand, FITC fluorescence intensities are decreased after exposure to the polycationic polymers in a concentration-dependent manner (Figure 9b). The largest amount of intensity

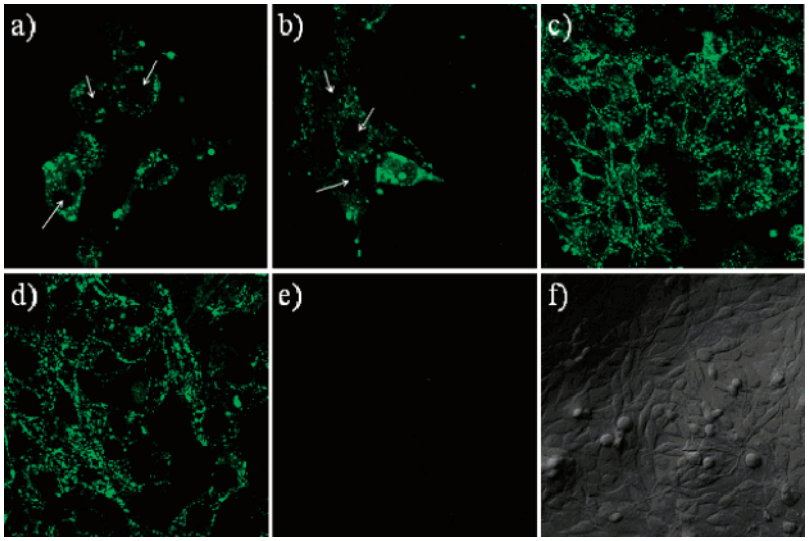

Figure 8. Confocal microscopy images of Rat2 cells incubated with (a) 6 μg/mL PLL−FITC and (b) 12 μg/mL PLL−FITC conjugates. (c) A zoomed-out image of b. Rat2 cells incubated with (d) 6 μg/mL G5-NH_2−FITC and (e) 12 μg/mL G5-Ac−FITC conjugates. (f) Differential interference contrast (DIC) image. Image f illustrates that there are a sufficient number of cells at the focal plane although nothing can be seen in fluorescence image e. Note that the green fluorescence from either PLL−FITC or G5-NH_2−FITC does not occur from within cell nuclei which are indicated by several white arrows. The location of the nuclei and the exclusion of the polycationic polymers were confirmed in previously published work using DAPI staining of the nucleus (*15*).

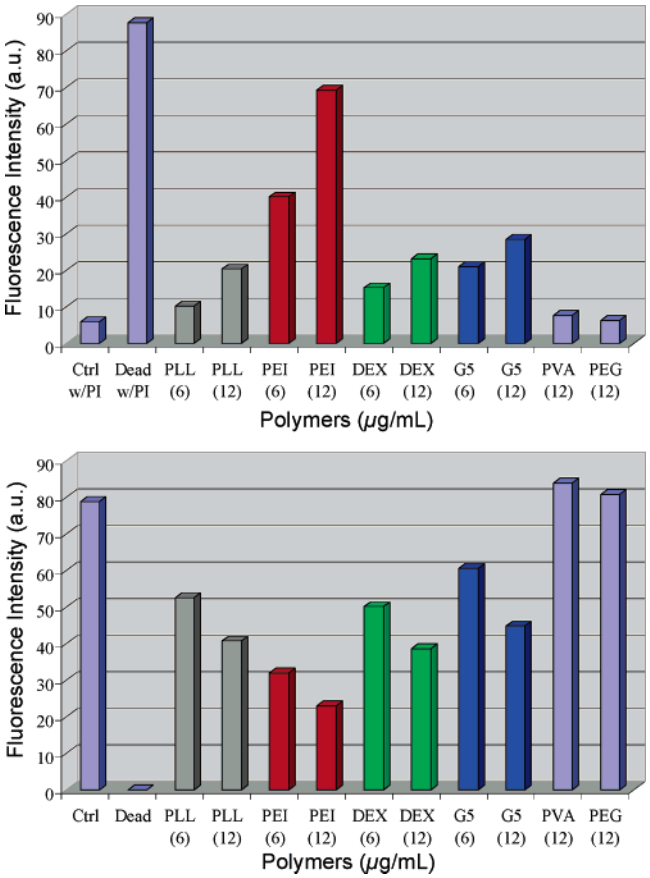

Figure 9. Fluorescence intensity of (a) propidium iodide (PI) and (b) fluorescein (FITC) from KB cells measured by flow cytometer. Note that fluorescence intensity of PI should increase while that of FITC should decrease with increase of membrane permeability. All the polycationic polymers cause an increase of PI fluorescence intensities and a decrease of FITC fluorescence. However, the neutral polymers do not cause such changes.

drop is observed in the PEI case, although DEAE-DEX, PLL, and G5 also show a decrease in FITC fluorescence intensity. As expected, PVA and PEG do not induce FITC escape.

DISCUSSION

Evidence for Hole Formation by Polycationic Polymers PEI, PLL, and DEAE-DEX. We previously reported nanoscale hole formation on both supported lipid bilayers and cellular membranes induced by positively charged PAMAM dendrimers (*15*−*19*). In this study we test the possibility of extending the proposed mechanism of dendrimer/membrane interactions, i.e., hole formation by sphere-like PAMAM dendrimers, to the more common and inexpensive polycationic polymers PEI, PLL, and DEAE-DEX. Polycationic polymer-induced disruption of various supported phospholipid bilayers including dioleoyl phosphatidyl choline (DOPC), dioleoyl phosphatidyl serine (DOPS), 1-palmitoyl-2-oleoyl-sn-glycero-3-phosphatidic acid (POPA), and their mixtures has been reported using various methods. These techniques include quartz crystal microbalance with dissipation, leakage assay, ^{31}P NMR, and electrophoretic mobility (*9*, *10*, *24*). Furthermore, polycationic polymer-induced permeabilization of living cell membranes has also been observed in vitro using enzyme assays and flow cytometry (*13*, *15*). In this paper, we correlate two separate types of studies (model membrane and in vitro studies) by performing simultaneous experiments at similar conditions to provide a better understanding of polymer/membrane interactions.

There are two basic types of disruption seen in AFM images: membrane hole formation and membrane thinning. 'Membrane hole formation' is the complete removal of the lipid bilayer from the mica surface, resulting in defects of 4 to 5 nm in depth. The apparent discrepancy between the expected depth for a removal of a full bilayer, 5 nm, and the depths experimentally measured in this study can be explained by the varying degrees of polymer adsorption to the surface of the mica. 'Membrane thinning', which could result from the reorientation of lipids or the removal of a layer of lipid from the lipid bilayer, yields depressions ranging between approximately 2 and 3 nm (*25*−*28*).

Although the effect of each of the polymers used in the study varies in degree, each of these commercial polycationic polymers induce disruption of the bilayers as shown in the AFM images (Figures 2−4). This study is consistent in terms of observing bilayer disruption but differs in both the type of disruption and concentration dependence as compared with the previous studies which examined the interaction of positively charged dendrimers

with a DMPC-supported lipid bilayers (*16*). Our in vitro study shows enzyme (LDH with MW 135−140 kDa and ∼4.3 nm in radius and LUC with MW 61 kDa and ∼2.7 nm in radius) leakage out of the cells, polymer internalization into the cells, and diffusion in and out of small molecular probes (PI and FITC respectively) through the living cell membranes (Figures 6−9) which are also consistent with our previous report using cationic PAMAM dendrimers (*15*). Therefore, it is clear that PEI, PLL, and DEAE-DEX also cause the formation of defects in both supported lipid bilayers and cell membranes.

Relationship between Polymer Properties and Membrane Permeabilization. As modern biotechnology tends toward the adaptation of biocompatible polymers for advanced biomedical applications, a fundamental understanding of these polymers, particularly in physiological conditions, should be obtained. In this paper, we try to provide a better understanding of the relationship between physical properties of polymers and biological membranes. GPC measurement enables us to rank hydrodynamic radii of the polycationic polymers in the following order: DEAE-DEX > PEI > PLL > G5 PAMAM. According to our AFM and in vitro studies, however, the size of the polymers does not seem to markedly affect their ability to induce hole formation in the membranes. Instead, it was found that the degree of membrane permeability is strongly dependent on the number of formal charges on the polymer chain. As shown in Table 1, PEI has the greatest density of charged groups on its single polymeric chain among the polymers used in this study. Not surprisingly, a significantly high amount of LDH and LUC was released in both cell lines after incubation with PEI. Furthermore, changes in fluorescence in PI and FITC as a result of interactions between PEI and cells were greater than changes induced by the other polycationic polymers. This indicates that charge interactions play a key role in inducing changes of membrane permeability, i.e., nanoscale hole formation. Our data on PLL, DEAE-DEX, and G5-NH_2, however, suggests that electrostatic interactions are not the only factor contributing to the effectiveness of polymer-induced nanoporation. Although PLL has an order of magnitude higher charge/monomer ratio than DEAE-DEX and G5-NH_2, the difference among those polymers in terms of enzyme leakage, PI internalization, and FITC escape is not remarkable. One possible explanation is that efficacy of hole formation is dependent on the architecture of polymers. That is, sphere-like (PAMAM), branched (PEI), or ring-containing (DEAE-DEX) molecular structures are likely more effective than linear polymers (PLL) at increasing membrane permeability. Mecke et al. also suggested that the macromolecular architecture is an important factor in the polymer/membrane interactions (*16*).

Taken as whole, it is found that the common, commercial polycationic polymers PEI, PLL, and DEAE-DEX result in the formation of defects on supported lipid bilayers, enzyme leakage out of cells, polymer internalization into cells, and diffusion in and out of small molecular probes (PI and FITC) through cell membranes. Our results directly support our hypotheses: (1) commercially available polycationic polymers, PEI, PLL, and DEAE-DEX cause nanoscale hole formation in supported lipid bilayers, (2) commercially available polycationic polymers, PEI, PLL, and DEAE-DEX cause substantial permeability of the cell plasma membrane leading to enzyme and dye diffusion, and (3) charge-neutral linear polymers do not induce hole formation in supported lipid bilayers or induce a significant change in membrane permeability. The proposed hypotheses are also consistent with our previous study using PAMAM dendrimers (*15*). An interesting addition to hypothesis 1 was raised by the DEAE-DEX experiments showing membrane thinning. Polycationic polymers appear capable of both nanoscale hole formation and membrane thinning events. Our data suggest that these polycationic polymer agents may be internalized into cells through the nanoscale holes generated in the membranes and that this is also a route of internalization for other materials.

In summary, we directly observe that polycationic polymers induce hole formation in supported lipid bilayers. Our in vitro results showing that polycationic polymers permeabilize living cell membranes allowing for the diffusion of molecules in and out, are consistent with a hole-formation mechanism (*15*, *16*). Once the concentration is above the nontoxic range (up to ∼12 μg/mL), the polymers cause substantial membrane damage resulting in cell death. From this point of view, these polycationic polymers are not ideal as biocompatible drug or gene delivery agents. Instead, charge-neutral polymers that do not cause nanoscale hole formation and cell membrane permeabilization would likely serve as a better choice when paired with a targeting moiety (*29*−*31*).

ACKNOWLEDGMENT

This project has been funded with federal funds from the National Cancer Institute, National Institutes of Health, under contract no. N01-CO-27173.

LITERATURE CITED

(1) Cho, Y. W., Kim, J. D., and Park, K. (2003) Pollycation gene delivery systems: escape from endosomes to cytosol. *J. Pharm. Pharmacol. 55*, 721−734.

(2) Davis, M. E. (2002) Nonviral gene delivery systems. *Curr. Opin. Biotechnol. 13*, 128−131.

(3) Segura, T., and Shea, L. D. (2001) Materials for nonviral gene delivery. *Annu. Rev. Mater. Res. 31*, 25−46.

(4) Rolland, A. P. (1998) From genes to gene medicines: Recent advances in nonviral gene delivery. *Crit. Rev. Ther. Drug 15*, 143−198.

(5) Behr, J. P. (1993) Synthetic Gene-Transfer Vectors. *Acc. Chem. Res. 26*, 274−278.

(6) Boussif, O., Lezoualch, F., Zanta, M. A., Mergny, M. D., Scherman, D., Demeneix, B., and Behr, J. P. (1995) A Versatile Vector For Gene And Oligonucleotide Transfer Into Cells In Culture And In−Vivo − Polyethylenimine. *Proc. Natl. Acad. Sci. U.S.A. 92*, 7297−7301.

(7) Kopatz, I., Remy, J. S., and Behr, J. P. (2004) A model for nonviral gene delivery: through syndecan adhesion molecules and powered by actin. *J. Gene Med. 6*, 769−776.

(8) Purohit, G., Sakthivel, T., and Florence, A. T. (2001) Interaction of cationic partial dendrimers with charged and neutral liposomes. *Int. J. Pharm. 214*, 71−76.

(9) Yaroslavov, A. A., Kuchenkova, O. Y., Okuneva, I. B., Melik-Nubarov, N. S., Kozlova, N. O., Lobyshev, V. I., Menger, F. M., and Kabanov, V. A. (2003) Effect of polylysine on transformations and permeability of negative vesicular membranes. *BBA-Biomembranes 1611*, 44−54.

(10) Zhang, Z. Y., and Smith, B. D. (2000) High-generation polycationic dendrimers are unusually effective at disrupting anionic vesicles: Membrane bending model. *Bioconjugate Chem. 11*, 805−814.

(11) Karoonuthaisiri, N., Titiyevskiy, K., and Thomas, J. L. (2003) Destabilization of fatty acid-containing liposomes by. polyamidoamine dendrimers. *Colloid. Surface. B 27*, 365−375.

(12) Kozlova, N. O., Bruskovskaya, I. B., Okuneva, I. B., Melik-Nubarov, N. S., Yaroslavov, A. A., Kabanov, V. A., and Menger, F. M. (2001) Interaction of a cationic polymer with negatively charged proteoliposomes. *BBA-Biomembranes 1514*, 139−151.

(13) Fischer, D., Li, Y. X., Ahlemeyer, B., Krieglstein, J., and Kissel, T. (2003) In vitro cytotoxicity testing of polycations: influence of polymer structure on cell viability and hemolysis. *Biomaterials 24*, 1121−1131.

(14) Benns, J. M., Mahato, R. I., and Kim, S. W. (2002) Optimization of factors influencing the transfection efficiency of folate-PEG-folate-graft-polyethylenimine. *J. Controlled Release 79*, 255−269.

(15) Hong, S., Bielinska, A. U., Mecke, A., Keszler, B., Beals, J. L., Shi, X. Y., Balogh, L., Orr, B. G., Baker, J. R., and Banaszak Holl,

M. M. (2004) Interaction of poly(amidoamine) dendrimers with supported lipid bilayers and cells: Hole formation and the relation to transport. *Bioconjugate Chem. 15*, 774−782.

(16) Mecke, A., Uppuluri, S., Sassanella, T. M., Lee, D.-K., Ramamoorthy, A., Baker, J. R., Orr, B. G., and Banaszak Holl, M. M. (2004) Direct Observation of Lipid Bilayer Disruption by Polyamidoamine Dendrimers. *Chem. Phys. Lipids 132*, 3−14.

(17) Mecke, A., Lee, D. K., Ramamoorthy, A., Orr, B. G., and Banaszak Holl, M. M. (2005) Membrane thinning due to antimicrobial peptide binding: An atomic force microscopy study of MSI-78 in lipid bilayers. *Biophys. J. 89*, 4043−4050.

(18) Mecke, A., Lee, D. K., Ramamoorthy, A., Orr, B. G., and Banaszak Holl, M. M. (2005) Synthetic and natural polycationic polymer nanoparticles interact selectively with fluid-phase domains of DMPC lipid bilayers. *Langmuir 21*, 8588−8590.

(19) Mecke, A., Majoros, I. J., Patri, A. K., Baker, J. R., Banaszak Holl, M. M., and Orr, B. G. (2005) Lipid bilayer disruption by polycationic polymers: The roles of size and chemical functional group. *Langmuir 21*, 10348−10354.

(20) Mecke, A., Lee, I., Baker, J. R., Banaszak Holl, M. M., and Orr, B. G. (2004) Deformability of poly(amidoamine) dendrimers. *Eur. Phys. J. E 14*, 7−16.

(21) Bielinska, A., KukowskaLatallo, J. F., Johnson, J., Tomalia, D. A., and Baker, J. R. (1996) Regulation of in vitro gene expression using antisense oligonucleotides or antisense expression plasmids transfected using starburst PAMAM dendrimers. *Nucleic Acids Res. 24*, 2176−2182.

(22) Bielinska, A. U., KukowskaLatallo, J. F., and Baker, J. R. (1997) The interaction of plasmid DNA with polyamidoamine dendrimers: mechanism of complex formation and analysis of alterations induced in nuclease sensitivity and transcriptional activity of the complexed DNA. *BBA-Gene Struct. Expr. 1353*, 180−190.

(23) Umebayashi, Y., Miyamoto, Y., Wakita, M., Kobayashi, A., and Nishisaka, T. (2003) Elevation of plasma membrane permeability on laser irradiation of extracellular latex particles. *J. Biochem. 134*, 219−224.

(24) Rossetti, F. F., Reviakine, I., Csucs, G., Assi, F., Voros, J., and Textor, M. (2004) Interactions between poly(L-Lysine)-*g*-poly(ethylene glycol) and Supported Phospholipid Bilayers. *Biophys. J. 86*, 174A−174A.

(25) Harroun, T. A., Heller, W. T., Weiss, T. M., Yang, L., and Huang, H. W. (1999) Experimental evidence for hydrophobic matching and membrane-mediated interactions in lipid bilayers containing gramicidin. *Biophys. J. 76*, 937−945.

(26) Heller, W. T., Waring, A. J., Lehrer, R. I., Harroun, T. A., Weiss, T. M., Yang, L., and Huang, H. W. (2000) Membrane thinning effect of the beta-sheet antimicrobial protegrin. *Biochemistry 39*, 139−145.

(27) Ludtke, S., He, K., and Huang, H. (1995) Membrane thinning caused by magainin 2. *Biochemistry 34*, 16764−16769.

(28) Mazzuca, C., Stella, L., Venanzi, M., Formaggio, F., Toniolo, C., and Pispisa, B. (2005) Mechanism of membrane activity of the antibiotic trichogin GA IV: A two-state transition controlled by peptide concentration. *Biophys. J. 88*, 3411−3421.

(29) Quintana, A., Raczka, E., Piehler, L., Lee, I., Myc, A., Majoros, I., Patri, A. K., Thomas, T., Mule, J., and Baker, J. R. (2002) Design and function of a dendrimer-based therapeutic nanodevice targeted to tumor cells through the folate receptor. *Pharm. Res. 19*, 1310−1316.

(30) Kukowska-Latallo, J. F., Candido, K. A., Cao, Z. Y., Nigavekar, S. S., Majoros, I. J., Thomas, T. P., Balogh, L. P., Khan, M. K., and Baker, J. R. (2005) Nanoparticle targeting of anticancer drug improves therapeutic response in animal model of human epithelial cancer. *Cancer Res. 65*, 5317−5324.

(31) Thomas, T. P., Patri, A. K., Myc, A., Myaing, M. T., Ye, J. Y., Norris, T. B., and Baker, J. R. (2004) In vitro targeting of synthesized anti body-conjugated dendrimer nanoparticles. *Biomacromolecules 5*, 2269−2274.

BC060077Y